ELSEVIER

Earth and Planetary Science Letters 164 (1998) 345–352

EPSL

Melt–peridotite reaction recorded in the chemistry of spinel and melt inclusions in basalt from 43ºN, Mid-Atlantic Ridge

Vadim Kamenetsky *, Anthony J. Crawford

School of Earth Sciences and Centre for Ore Deposit Research, University of Tasmania, GPO Box 252-79, Hobart, Tasmania, 7001, Australia

Received 28 April 1998; revised version received 12 August 1998; accepted 11 September 1998

Abstract

Compositions of spinel and glassy melt inclusions in primitive olivine ($Fo_{89.3–91}$) from basalt AII32 D11-177 at 43ºN, Mid-Atlantic Ridge fall into two principal groups. The dominant (~90%) Group-I spinel and melt inclusions have typical MORB compositions. In contrast, Group-II Cr-spinels are strongly enriched in TiO_2 (2.6–4.1 wt%), and Group-II melt inclusions show significant enrichment in SiO_2 (54.6–58.4 wt%), TiO_2, Na_2O and K_2O, whereas their CaO contents (9.3–11.1 wt%) are unusually low. Group-II melts are also remarkable in crystallizing high-Mg orthopyroxene (Mg# 91). These mineral associations and melt compositions are unusual for MORB, and are interpreted to result from interaction between MORB-like melts and harzburgitic peridotite at low pressure.

Keywords: mid-ocean ridge basalts; melts; inclusions; spinel; peridotites; petrology

1. Introduction

Reaction between an ascending melt and wallrock peridotite beneath mid-ocean spreading centers, an idea originally developed from the study of ophiolites (e.g., [1–6]), has gained additional support from chemical 'refertilization' trends in abyssal peridotites [7]. The recent discovery within refractory mantle rocks of tabular to irregular bodies of dunite containing melt impregnations in the form of gabbros and troctolites in a number of localities in Atlantic and Pacific oceans [8–13], allowed preliminary assessments of the nature and extent of phase modifications in peridotites. The record of melt–peridotite interaction is best shown by compositions of the mineral constituents of these rocks, which are believed to be the reaction products [9–11,14], and also by the presence of hydrous phases included in spinel in dunites and troctolites [8,15].

Despite the recent evaluation of effects of melt–harzburgite interaction during petrogenesis of Hawaiian intraplate tholeiitic magmas [16], the consequences of the reaction between percolating melt and upper mantle peridotite on MORB compositions is not as yet well constrained. Therefore, further research into diverse melt fractions that may have escaped shallow-level mixing is warranted in order to understand the compositions of MORB primary melts, their evolutionary paths during ascent and the effects of high-pressure fractionation and re-equilibration on the compositions of residual peridotites

* Corresponding author. Tel.: +613 6226 7649; Fax: +613 62232547; E-mail: dima.kamenetsky@utas.edu.au

0012-821X/98/$ – see front matter
PII: S0012-821X(98)00226-X

and erupted rocks and glasses. This will better constrain understanding of mechanisms of melt transport through the upper mantle and help to refine models for the formation of the oceanic crust.

In this paper we present the results of detailed study of mineral and melt inclusion compositions in basaltic rocks (MORB) from 43ºN, Mid-Atlantic Ridge. The unusual chemistry of melts and liquidus phases is interpreted to arise from melt–peridotite interaction and reflect the evolutionary trends of common MORB melts during this interaction. These data complement our previous discovery of primitive clinopyroxene phenocrysts and high-Ca melt inclusions in basalt AII32 D12-7 from the same locality [17].

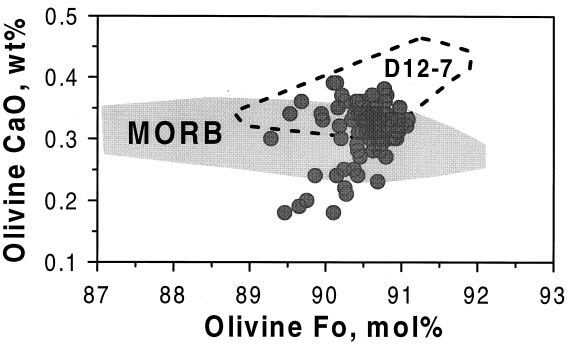

Fig. 1. Composition of olivine phenocrysts in basalt AII32 D11-177 in comparison with typical MORB olivine compositions and olivines from sample AII32 D12-7 [17]. Note, that olivines from 43ºN MAR are among the most primitive MORB compositions, and their CaO abundances are suggestive of crystallization from a range of melts both more depleted and more enriched in CaO than common MORB.

2. Phenocrysts and melt inclusions in sample AII-32 D11-177

Sample AII32 D11-177 was dredged during cruise 32 of the R/V Atlantis II from 1983–2168 m water depth in the eastern part of the median valley of the Mid-Atlantic Ridge (MAR) at 42º57′N 29º15′W [18,19]. This area is a 'normal' ridge segment adjacent to the 43ºN fracture zone on the periphery of the Azores Platform, and is characterized by normal to enriched MORB tholeiitic magmatism [17,19] and particularly refractory abyssal peridotites [20,21].

The sample is a glassy olivine-phyric basalt (olivine ~10–15 vol%) with quenched pillow-rim glass. The glass has a primitive major element composition with Mg# = 69.7 and CaO/Al_2O_3 = 0.86 (Table 1), and is enriched in K_2O, H_2O (0.49 wt%) and other highly incompatible elements (e.g., La/Yb = 3.7), thus having affinities with E-MORB. Olivine phenocrysts (up to 4 mm in size) range from $Fo_{89.3}$ to Fo_{91}, and they contain abundant inclusions of spinel and glass. Their CaO contents are more variable (0.18–0.4 wt%) than expected for a single fractionation-related population of magnesian olivine (Fig. 1).

Table 1
Compositions of pillow-rim glass and mineral and melt inclusions in olivine from basalt AII-32 D11-177

	1	2	3	4	5	6	7	8
SiO_2	50.95	49.30	50.50	54.97	58.42	57.29	n.d.	n.d.
TiO_2	0.93	0.98	1.09	2.08	1.95	0.29	0.42	3.15
Al_2O_3	15.60	15.48	16.92	14.54	14.99	1.22	20.16	28.67
FeO	7.82	7.65	7.58	7.45	5.28	6.01	15.19	18.52
MgO	9.10	8.32	5.44	7.32	5.37	34.24	15.77	18.04
CaO	13.39	14.35	14.84	10.36	9.33	1.55	n.d.	n.d.
Na_2O	2.00	1.74	2.00	2.32	2.90	0.02	n.d.	n.d.
K_2O	0.25	0.44	0.35	1.12	0.99	n.d.	n.d.	n.d.
Cr_2O_3	n.d.	n.d.	n.d.	n.d.	n.d.	0.40	47.24	31.42
Fo host		90.40	90.53	89.86	90.10	90.76	90.79	89.65

1 = pillow-rim glass; 2, 3 and 7 = Group-I ('common' MORB) melt and spinel inclusions, respectively; 4, 5 and 8 = Group-II melt and spinel inclusions, respectively; 6 = orthopyroxene inclusions, associated with Group-II glass (Fig. 6). 4 and 8 = melt and spinel inclusions coexisting in the same olivine grain #23 (see text and Fig. 5).
All oxides in wt%, Fo in mol%. n.d. — not determined.

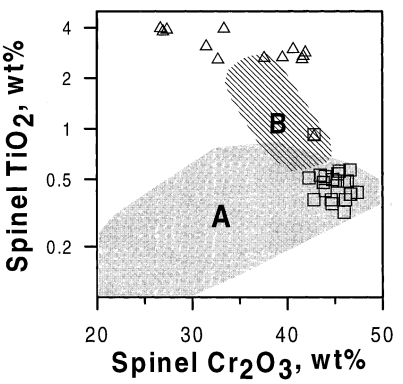

Fig. 2. Compositions (Cr_2O_3 and TiO_2, in wt%) of spinel inclusions (*squares*, Group-I; *triangles*, Group-II) in olivine. Spinels in mid-oceanic basalts (field A, our unpublished data and [22–24]) and in melt impregnated mantle rocks from Hess Deep and Garrett Transform fault (field B, [8–10,13–15,25]) are shown for comparison.

Compositions of spinel inclusions (Table 1) fall into two principal groups based on their TiO_2 (0.32–0.57 wt% in Group-I (85%), 2.6–4.1 wt% in Group-II (15%)) and Cr_2O_3 (42.2–47.2 and 26.6–41.8, respectively) contents (Fig. 2), with one intermediate composition (TiO_2 0.92 wt%). Group-II spinels also have higher Al_2O_3 (21–29.3) and Fe_2O_3 (5.1–8.8) than Group-I spinels (19.8–23.2 and 4–6.2 wt%, respectively), and are hosted by statistically less magnesian olivine (average Fo: 90.1 vs. 90.7). Note that extremely high TiO_2 compositions of Group-II spinel are atypical of MORB, and suggest unusual parental melt compositions.

Compositions of glassy melt inclusions can also be subdivided into two groups (Fig. 3, Table 1). Group-I glasses are more evolved than pillow-rim glass in terms of their MgO contents (3–8.5 wt%), and their compositional trends are broadly consistent with crystallization of olivine (Fo $<$ 90) on the inclusion walls. When corrected for olivine fractionation, they have typical MORB compositions and are similar to the pillow-rim glass, though the latter has notably higher SiO_2 and Na_2O. In contrast, Group-II melt inclusion compositions (10% in total) are unusual in having abnormally high SiO_2 (54.6–58.4 wt%) and low CaO (9.3–11.1 wt%) contents, and in comparison with Group-I inclusions their TiO_2, Na_2O and K_2O contents are higher, but Al_2O_3 is lower (Fig. 3). The spread in Group-II compositions is not related to processes of post-entrapment modification caused by olivine fractionation (Fig. 2, e.g., MgO vs. CaO). Furthermore, these inclusions are hosted by olivine whose Fo ($<$90.2) and CaO ($<$0.24 wt%) values are at the lowest end of the compositional arrays, whereas Group-I high CaO/Al_2O_3 melt inclusions associate exclusively with high-Ca ($>$0.27 wt%) olivine (Fig. 4).

The relation between melt and spinel inclusion compositional groups is examined in Fig. 5. Individual compositions of melt and spinel inclusions, which are trapped in different olivine phenocrysts, define wide ranges of TiO_2/Al_2O_3 (Group-I and Group-II compositions). Two glass inclusions and one spinel inclusion (Group-II), coexisting in the same olivine grain #23 (Table 1, NN 4 and 8) are plotted inside coordinates. The compositions of homogenized melt inclusions trapped in spinel from samples D11-92 and D12-2 (same locality) are also plotted as a guide to the equilibrium chemistry of coexisting melt and spinel in this system. They are best approximated by a second degree polynomial function ($R = 0.84$) which trends towards the high TiO_2/Al_2O_3 end of D11-177 array, passing through the composition of associated melt and spinel inclusions in olivine (grain #23). This implies that melt and spinel compositional groups described above are mutually correlated, and that the unusually high-Ti spinel compositions are a reflection of melt compositions enriched in Ti and depleted in Al.

Silica-enriched Group-II melt compositions are clearly saturated in orthopyroxene component, and might be expected to have orthopyroxene on the liquidus. A careful search located euhedral crystals of high-Mg (Mg# 91) orthopyroxene (Table 1, Fig. 6) in low-CaO (0.21 wt%) olivine in association with high-Si melt inclusions. To the best of our knowledge this is the second finding of orthopyroxene in MORB (see [27,28]).

3. Discussion

Common MORB minerals and melt inclusions in basalt D11-177 coexist with an atypical liquidus assemblage (~10–15%), comprising primitive low-Ca olivine, high-Ti chromian spinel, orthopyroxene and melt enriched in Si, Ti, Na and K, and depleted

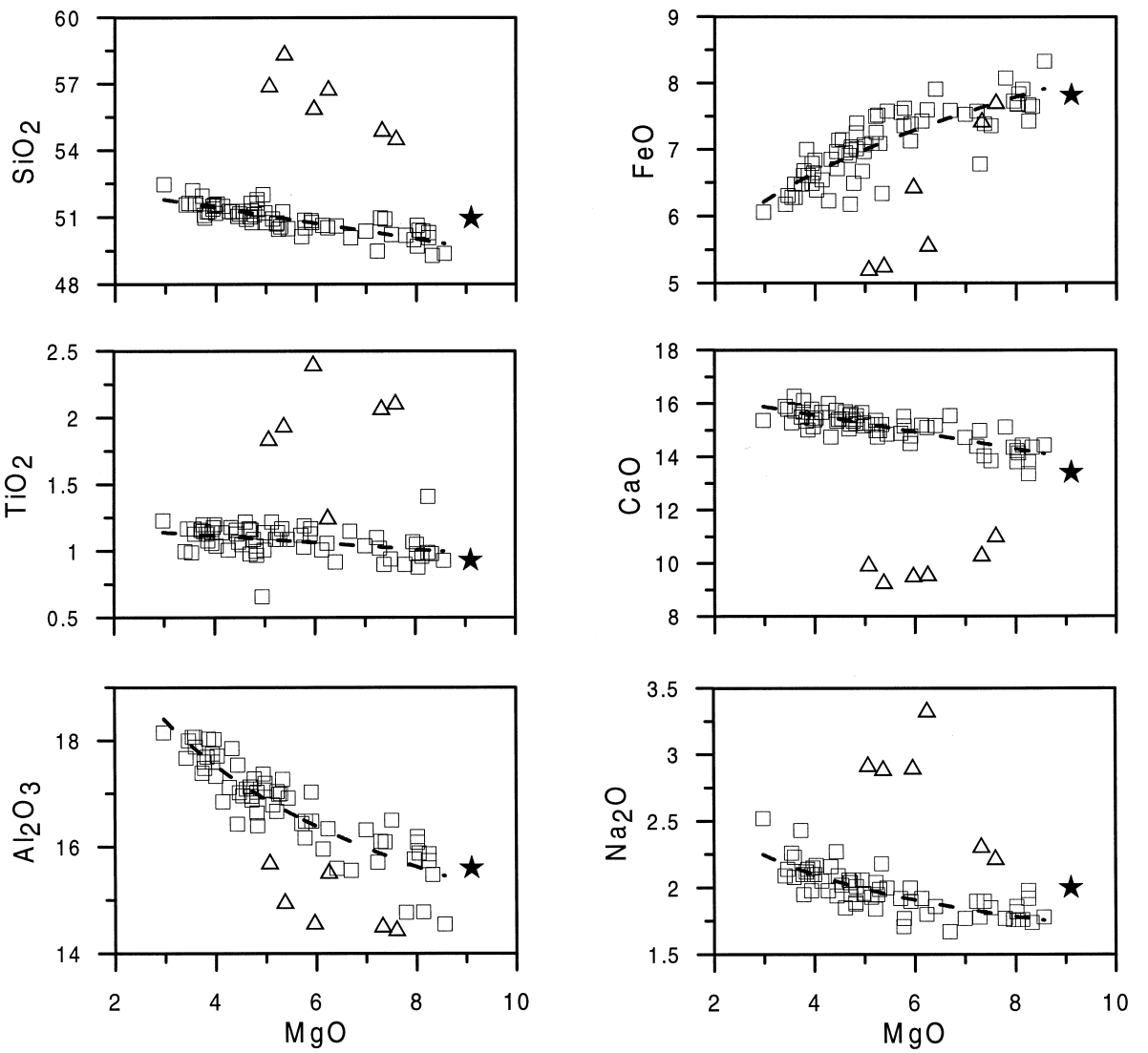

Fig. 3. Compositions of melt inclusions (*squares*, Group-I; *triangles*, Group-II) in olivine and AII-32 D11-177 pillow-rim glass (*star*). Oxides in wt%.

in Al and Ca. The record of diverse mineral and melt inclusion compositions within a single MORB sample is not uncommon (e.g., [17,24,28]), but in this case the compositional groups cannot be directly linked by mantle melting or magma chamber fractionation processes. Previously, the rare presence of primitive orthopyroxene in DSDP Site 334 cumulates [29] and in a Vema fracture zone basalt in association with high-Si ultra-depleted (UDM) melt [27,28] was interpreted to result from crystallization of highly depleted magmas, formed by shallow level (<5 kbar) critical (continuous) melting of already depleted mantle peridotite. As these latest-stage, low-pressure fractional melts are very depleted in Ti and Na and have elevated Al contents [27,28] this could not be a viable explanation for our Group-II melt compositions. Note, that the composition of primitive orthopyroxene (Mg# 90.8) in association with the UDM [27,28] is quite different from the composition of orthopyroxene on

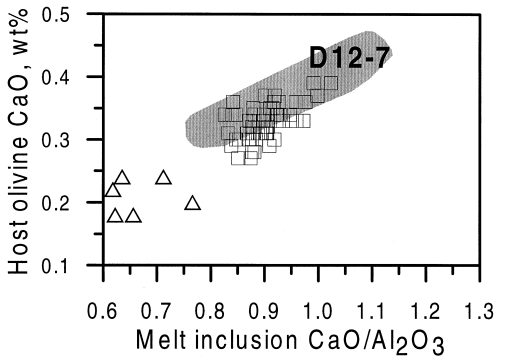

Fig. 4. Correlation between CaO/Al_2O_3 in melt inclusions and CaO of host olivines. Symbols as in Fig. 3. Compositions of high-Ca melt inclusions in olivine from basalt AII32 D12-7 [17], plotted as a field, can be considered complimentary to low-Ca Group-II melts.

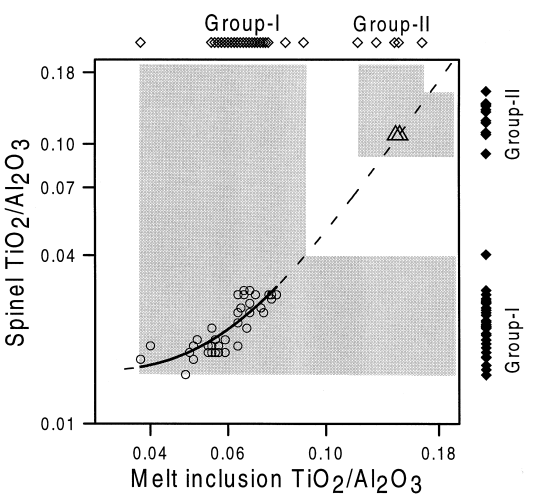

Fig. 5. Plot of TiO_2/Al_2O_3 in spinel inclusions vs. TiO_2/Al_2O_3 in melt inclusions hosted in primitive olivine ($Fo_{89.3–91}$) in basalt AII-32 D11-177. During sample preparation and analysis, only a single olivine grain (#23) showed simultaneous exposure at the grain surface of both one spinel and two melt inclusions; these are plotted as *triangles*. In other olivines, melt inclusions (*open diamonds*) or only spinels (*closed diamond*) but never both, were exposed in any individual grain, precluding plotting any more compositional pairs in this diagram. To provide further data, we have analysed homogenized melt inclusions in spinel phenocrysts in two other MORB from the same locality AII-32 D11-92 and AII-32 D12-2 (*circles*). Note the trend through the latter data (solid line) extrapolates (dotted line) to the Group-II spinel/melt compositions in grain #23 (Table 1, NN 4 and 8), and that compositions of other spinels and melt inclusions in our sample (plotted outside the diagram, as they occur in different olivine grains) can be projected (shaded areas) to define the same trend.

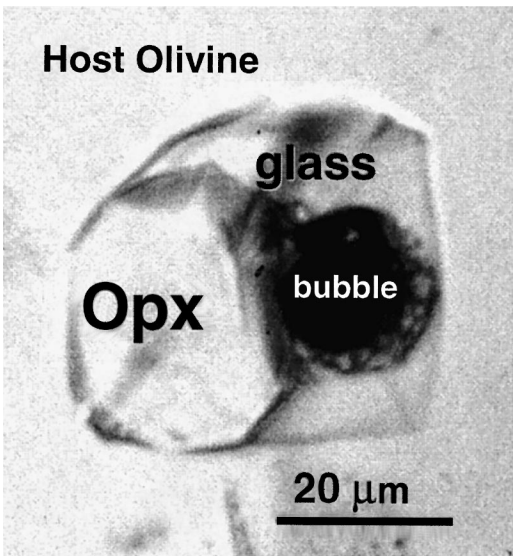

Fig. 6. Complex inclusion in forsteritic olivine ($Fo_{90.8}$) comprising orthopyroxene crystal (Table 1, N6), Group-II high-Si, low-Ca glass and fluid bubble. This orthopyroxene is compositionally different from orthopyroxene found in the ultra-depleted melt inclusion in Vema fracture zone basalt [27,28].

liquidus of Group-II melts (Table 1, N6) in having lower SiO_2 (55.3) and TiO_2 (0.04) and higher Al_2O_3 (2.1) and CaO (2.2). These diverse orthopyroxene compositions are in agreement with the contrasting compositional features of the UDM and D11-177 Group-II magmas and suggest different genesis.

We also note that our Group-II melt inclusions have some chemical affinities with Si-rich, Ca-poor alkaline glasses found in mantle xenoliths worldwide (see reviews in [30,31]), and Group-II spinels are much closer to Ti- and Fe^{3+}-rich chromites in some mantle rocks from Hess Deep and Garrett transform fault on the East Pacific Rise (EPR), than to MORB spinel (Fig. 2). What do these glass-hosting xenoliths and titaniferous spinel-bearing abyssal rocks have in common? They all demonstrate textural and chemical evidence of melt–peridotite reaction followed by extensive replacement of primary orthopyroxene by olivine + clinopyroxene + spinel ± plagioclase assemblages [11,12,31]. What features do the melt-impregnated peridotites from the EPR and 43°N MAR peridotites have in common? They all are Cpx-poor harzburgites with similar, most refractory compositions of residual phases [9–

13,20,25,32]. Moreover, 43ºN MAR peridotites, in contrast to the majority of porphyroclastic abyssal peridotites, have protogranular textures expressed by clinopyroxene and spinel occurring "at the peripheries of, interstitially between, or as irregular blebs in, the large orthopyroxene grains" [20]. Such a texture is commonly attributed to recrystallization processes in the mantle (e.g., [33,34]).

The notion of dissolution of pyroxene in olivine-saturated magmas [3] has been elaborated by Kelemen and coworkers (e.g., [26,35]), who discussed dissolution of orthopyroxene and concomitant precipitation of olivine and clinopyroxene during melt–peridotite interaction at constant or decreasing temperatures in the shallow mantle. Thus, the origin of clinopyroxene dunite or olivine-rich wehrlite mantle lithologies was explained by the reaction between basaltic magma saturated in olivine and calcic pyroxene and peridotite wall rocks. Similarly, orthopyroxene dissolution and concomitant crystallization of olivine and diopside has been demonstrated to result from reaction of ephemeral carbonatite magmas with lherzolitic lithospheric mantle [36]. Also, the presence of melt–peridotite interaction has usually been inferred from the compositions of abyssal and alpine peridotites. Our study links composition of melts and liquidus assemblage in erupted lavas with unusual 'recrystallization' features of upper mantle peridotites.

To explain the peculiar features (high Si, Ti, Na, K and low Ca and Al) of D11-177 Group-II melt inclusions we propose the following:

(1) 'typical' MORB liquids (e.g., with the composition of magmas parental to the Group-I melt inclusions) produced within lherzolitic mantle at high pressure segregate and commence ascent;

(2) these melts are saturated in olivine and undersaturated in orthopyroxene component at low pressure (e.g., [37,38]), and particularly at elevated H_2O abundances;

(3) some melt fractions react with the shallow wallrock harzburgitic mantle residual after MORB extraction, whereas others pass through unmodified;

(4) the reactive melts crystallize olivine, clinopyroxene, and an aluminous phase (spinel or possibly plagioclase if pressures <10 kbar) within harzburgite and dissolve orthopyroxene [11,12,15], and resultant melts are thus buffered at high 'mantle' Mg# values [26,35], whereas the abundances of Si increase and Ca and Al decrease. The observed enrichment of the Group-II melts in moderately incompatible Ti and Na argues for a decrease in the magma mass, i.e. amount of crystallizing phases exceeds the amount of orthopyroxene dissolving into melt;

(5) mixing of common MORB melts and the products of their interaction with harzburgite en route to the surface or in shallow magma chambers beneath the ridge may produce hybrid magmas with elevated Si and Na and reduced Ca abundance, similar to AII32 D11-177 pillow rim glass (Fig. 3);

(6) clinopyroxene-rich, orthopyroxene-poor mantle lithologies within shallow mantle peridotite are likely to be left behind as a result of melt–peridotite interaction outlined above.

Significant evidence for the formation of clinopyroxene-enriched peridotite during migration of 'typical' MORB melts comes from the study of mineralogy and melt inclusions in basalt AII32 D12-7 [17]. This rock was dredged from the same locality at the Mid-Atlantic Ridge as our sample AII32 D11-177, but at a shallower depth (1440–1820 m water depth), so it may be slightly younger. D12-7 is unusual in that it carries extremely primitive Cr-diopside (Mg# 90–92), high-Ca olivine (Fo up to 92, Fig. 1), and Cr-spinel (Cr# up to 70, cf. <60 in MORB) phenocrysts. The unusual mineral assemblage in this basalt is in excellent agreement with similarly atypical compositions of homogenized high-Mg (MgO 10–12 wt%) melt inclusions in olivine phenocrysts, which have high CaO (up to 15.2) and low Al_2O_3 (12.8–15.5), so their CaO/ Al_2O_3 value (Fig. 4) trends to very high values (up to 1.2 — cf., <0.9 in MORB). Because these melt compositions deviate strongly from 4-phase peridotite saturation and are saturated with olivine + clinopyroxene only, they have been earlier interpreted as the products either of melt–wallrock reaction between a MORB melt and clinopyroxene-rich lithology (e.g., wehrlite), or of mixing between melts derived separately from distinct mantle lithologies [17]. Therefore, our detailed mineralogical and melt inclusion data from basalts from 43ºN MAR provide additional insight into the mechanism of melt–peridotite interaction and subsequent effects on the composition of erupted MORB magmas.

Acknowledgements

Our special thanks go to Dr. Eugene Sabourenkov, who first discussed the unusual compositions of spinel with us, and encouraged this study. Dr. David Steele provided help with microprobe analyses. Two anonymous reviewers provided additional ground for discussion. This work is supported by the ARC Special Research Centers Program. ***[CL]***

References

[1] C.A. Evans, Magmatic metasomatism in peridotites from the Zambales ophiolite, Geology 13 (1985) 166–169.

[2] P.B. Kelemen, H.J.B. Dick, J.E. Quick, Formation of harzburgite by pervasive melt–rock reaction in the upper mantle, Nature 358 (1992) 635–641.

[3] J.E. Quick, The origin and significance of large, tabular dunite bodies in the Trinity Peridotite, northern California, Contrib. Mineral. Petrol. 78 (1981) 413–422.

[4] J.E. Quick, R.T. Gregory, Significance of melt–wall rock reaction: a comparative anatomy of three ophiolites, J. Geol. 103 (1995) 187–198.

[5] M. Rabinowicz, G. Ceuleneer, A. Nicolas, Melt segregation and flow in mantle diapirs below spreading centers: evidence from the Oman ophiolite, J. Geophys. Res. 92 (1987) 3475–3486.

[6] G. Suhr, P.T. Robinson, Origin of mineral chemical stratification in the mantle section of the Table Mountain massif (Bay of Islands Ophiolite, Newfoundland, Canada), Lithos 31 (1994) 81–102.

[7] D. Elthon, Chemical trends in abyssal peridotites: refertilization of depleted suboceanic mantle, J. Geophys. Res. 97 (1992) 9015–9025.

[8] S. Arai, K. Matsukage, Petrology of gabbro–troctolite–peridotite complex from Hess Deep, equatorial Pacific: implications for mantle–melt interaction within the oceanic lithosphere, in: C. Mevel, K.M. Gillis, J.F. Allan, P.S. Meyer (Eds.), Proc. ODP, Sci. Results 147 (1996) 135–155, Ocean Drilling Program, College Station, TX.

[9] M. Cannat, D. Bideau, R. Hébert, Plastic deformation and magmatic impregnation in serpentinized ultramafic rocks from the Garrett transform fault (East Pacific Rise), Earth Planet. Sci. Lett. 101 (1990) 216–232.

[10] H.J.B. Dick, J.H. Natland, Late-stage melt evolution and transport in the shallow mantle beneath the East Pacific Rise, in: C. Mevel, K.M. Gillis, J.F. Allan, P.S. Meyer (Eds.), Proc. ODP, Sci. Results 147 (1996) 103–134, Ocean Drilling Program, College Station, TX.

[11] S.J. Edwards, J. Malpas, Melt–peridotite interaction in shallow mantle at the East Pacific Rise: evidence from ODP Site 895 (Hess Deep), Mineral. Mag. 60 (1996) 191–206.

[12] J. Girardeau, J. Francheteau, Plagioclase-wehrlites and peridotites on the East Pacific Rise (Hess Deep) and the Mid-Atlantic Ridge (DSDP site 334): evidence for magma percolation in the oceanic upper mantle, Earth Planet. Sci. Lett. 115 (1993) 137–149.

[13] R. Hekinian, D. Bideau, J. Francheteau, J.L. Cheminee, R. Armijo, P. Lonsdale, N. Blum, Petrology of the East Pacific Rise crust and upper mantle exposed in Hess Deep (Eastern Equatorial Pacific), J. Geophys. Res. 98 (1993) 8069–8094.

[14] J.F. Allan, H.J.B. Dick, Cr-rich spinel as a tracer for melt migration and melt–wall rock interaction in the mantle: Hess Deep, Leg 147, in: C. Mevel, K.M. Gillis, J.F. Allan, P.S. Meyer (Eds.), Proc. ODP, Sci. Results 147 (1996) 157–172, Ocean Drilling Program, College Station, TX.

[15] S. Arai, K. Matsukage, E. Isobe, S. Vysotskiy, Concentration of incompatible elements in oceanic mantle: Effect of melt/wall interaction in stagnant or failed melt conduits within peridotite, Geochim. Cosmochim. Acta 61 (1997) 671–675.

[16] T.P. Wagner, T.L. Grove, Melt/harzburgite reaction in the petrogenesis of tholeiitic magma from Kilauea volcano, Hawaii, Contrib. Mineral. Petrol. 131 (1998) 1–12.

[17] V.S. Kamenetsky, S.M. Eggins, A.J. Crawford, D.H. Green, M. Gasparon, T.J. Falloon, Calcic melt Inclusions in primitive olivine at 43ºN MAR: Evidence for melt–rock reaction/melting involving clinopyroxene-rich lithologies during MORB generation, Earth Planet. Sci. Lett. 160 (1998) 115–132.

[18] J.D. Phillips, G. Thompson, R.P. von Herzen, V.T. Bowen, Mid-Atlantic ridge near 43º latitude, J. Geophys. Res. 74 (1969) 3069–3081.

[19] T. Shibata, G. Thompson, F.A. Frey, Tholeiitic and alkali basalts from the Mid-Atlantic Ridge at 43ºN, Contrib. Mineral. Petrol. 70 (1979) 127–141.

[20] T. Shibata, G. Thompson, Peridotites from the Mid-Atlantic Ridge at 43ºN and their petrogenetic relation to abyssal tholeiites, Contrib. Mineral. Petrol. 93 (1986) 144–159.

[21] E. Bonatti, P.J. Michael, Mantle peridotites from continental rifts to ocean basins to subduction zones, Earth Planet. Sci. Lett. 91 (1989) 297–311.

[22] J.F. Allan, R.O. Sack, R. Batiza, Cr-rich spinels as petrogenetic indicators: MORB-type lavas from the Lamont seamount chain, eastern Pacific, Am. Mineral. 73 (1988) 741–753.

[23] H.J.B. Dick, T. Bullen, Chromian spinel as a petrogenetic indicator in abyssal and alpine-type peridotites and spatially associated lavas, Contrib. Mineral. Petrol. 86 (1984) 54–76.

[24] V. Kamenetsky, Methodology for the study of melt inclusions in Cr-spinel, and implications for parental melts of MORB from FAMOUS area, Earth Planet. Sci. Lett. 142 (1996) 479–486.

[25] R. Hébert, D. Bideau, R. Hekinian, Ultramafic and mafic rocks from the Garrett Transform Fault near 13º30′S on the East Pacific Rise: igneous petrology, Earth Planet. Sci. Lett. 65 (1983) 107–125.

[26] P.B. Kelemen, G. Hirth, N. Shimizu, M. Spiegelman, H.J.B. Dick, A review of melt migration processes in the adiabatically upwelling mantle beneath oceanic spreading ridges, Philos. Trans. R. Soc. London A 355 (1997) 283–318.

[27] L.V. Danyushevsky, A.V. Sobolev, L.V. Dmitriev, Low-titanium orthopyroxene-bearing tholeiite, a new type of ocean-rift tholeiite, Trans. (Doklady) USSR Acad. Sci. 292 (1987) 102–105.
[28] A.V. Sobolev, N. Shimizu, Ultra-depleted primary melt included in an olivine from the Mid-Atlantic Ridge, Nature 363 (1993) 151–154.
[29] K. Ross, D. Elthon, Cumulates from strongly depleted mid-ocean-ridge basalt, Nature 365 (1993) 826–829.
[30] P. Schiano, R. Clocchiatti, Worldwide occurrence of silica-rich melts in sub-continental and sub-oceanic mantle minerals, Nature 368 (1994) 621–624.
[31] G.M. Yaxley, V. Kamenetsky, D.H. Green, T.J. Falloon, Glasses in mantle xenoliths from western Victoria, Australia, and their relevance to mantle processes, Earth Planet. Sci. Lett. 148 (1997) 433–446.
[32] Y. Niu, R. Hekinian, Basaltic liquids and harzburgitic residues in the Garrett Transform: a case study at fast-spreading ridges, Earth Planet. Sci. Lett. 146 (1997) 243–258.
[33] J.-C.C. Mercier, A. Nicolas, Textures and fabrics of upper-mantle peridotites as illustrated by xenoliths from basalts, J. Petrol. 16 (1975) 454–487.
[34] A. Nicolas, F. Boudier, J.-L. Bouchez, Interpretation of peridotite structures from ophiolitic and oceanic environments, Am. J. Sci. 280 (1980) 192–210.
[35] P.B. Kelemen, Reaction between ultramafic wall rock and fractionating basaltic magma I. Phase relations, the origin of calc-alkaline magma series, and the formation of discordant dunite, J. Petrol. 31 (1990) 51–98.
[36] G.M. Yaxley, A.J. Crawford, D.H. Green, Evidence for carbonatite metasomatism in spinel peridotite xenoliths from western Victoria, Australia, Earth Planet. Sci. Lett. 107 (1991) 305–317.
[37] A.L. Jaques, D.H. Green, Anhydrous melting of peridotite at 0–15 kb pressure and the genesis of tholeiitic basalts, Contrib. Mineral. Petrol. 73 (1980) 287–310.
[38] E. Stolper, A phase diagram for mid-ocean ridge basalts: preliminary results and implications for petrogenesis, Contrib. Mineral. Petrol. 74 (1980) 13–27.